

Scaling in back-illuminated GaN avalanche photodiodes

K. Minder, J. L. Pau, R. McClintock, P. Kung, C. Bayram, and M. Razeghi^{a)}
 Center for Quantum Devices, Department of Electrical Engineering and Computer Science,
 Northwestern University, Evanston, Illinois 60208

D. Silversmith

Air Force Office of Scientific Research, Arlington, Virginia 22203

(Received 10 May 2007; accepted 25 July 2007; published online 15 August 2007)

Avalanche *p-i-n* photodiodes of various mesa areas were fabricated on AlN templates for back illumination for enhanced performance through hole-initiated multiplication, and the effects of increased area on device performance were studied. Avalanche multiplication was observed in mesa sizes up to $14\,063\ \mu\text{m}^2$ under linear mode operation. Uniform gain and a linear increase of the dark current with area were demonstrated. © 2007 American Institute of Physics.

[DOI: 10.1063/1.2772199]

Ultraviolet (UV) photodetectors find uses in numerous applications in the defense, commercial, and scientific arenas. GaN and AlGaIn avalanche photodiodes (APDs) present themselves as particularly strong candidates for reliable UV detection, providing a promising replacement for bulky and fragile photomultiplier tubes. Their direct and tunable wide band gap, intrinsic rejection of the visible spectrum, and high bond strength are important advantages over competing technologies. However, numerous material-, fabrication-, and design-related issues remain before GaN APDs can be commercialized.

Although there have been reports on the development and characterization of (Al)GaIn *p-i-n* APDs,^{1–4} as well as a few AlGaIn Schottky APDs,⁵ most of them have been limited to small area devices, generally less than $3000\ \mu\text{m}^2$, primarily operated under front illumination. By contrast, back illumination allows easier integration and packaging through flip-chip technology as required for the production of APD arrays;⁶ in addition, back illumination favors hole-initiated multiplication, which we have found yields superior gain and noise characteristics.⁷ In this work, we report on the growth, fabrication, and characterization of back-illuminated *p-i-n* GaN APDs of various mesa areas.

p-i-n samples were grown in an Aixtron 200/4-HT metal-organic chemical vapor deposition reactor on double-sided polished sapphire substrates. The template consists of 500 nm of high-quality AlN grown atop a 20 nm low-temperature AlN nucleation layer, similar to that discussed in our previous papers.⁸ The device structure consists of a 200 nm GaN:Si *n*-type region, followed by a 200 nm unintentionally doped GaN *i* region, and capped with a 285 nm GaN:Mg *p*-type region. Carrier concentrations in these layers were estimated by Hall-effect measurement of test samples yielding values in the $(1-2) \times 10^{16}$ and $(1-2) \times 10^{18}\ \text{cm}^{-3}$ for the electron concentrations in the *i*-GaN and *n*-GaN layers, respectively, and $(1-3) \times 10^{18}\ \text{cm}^{-3}$ for the hole concentration in the *p*-GaN layer. Following growth and characterization, various sized mesas ranging in area from 225 to $25\,000\ \mu\text{m}^2$ were defined via photolithography and dry etching. A thin Ni/Au (30 Å/30 Å) *p*-type contact was then deposited and annealed, followed by the deposition of

Ti/Au (400 Å/1200 Å) for a *n*-type Ohmic contact and as a protective contact layer over the thin Ni/Au contact. Finally, a 300 nm SiO₂ passivation layer was deposited, and windows were opened in order to contact the devices for testing.

The electric field in the device as a function of reverse bias and the normalized absorption probability for an absorption coefficient of $10^5\ \text{cm}^{-1}$ were modeled to give insight into device operation.⁹ An electric field of 3.0 MV/cm at breakdown was calculated, close to previously reported experimental values,⁷ while the relative absorption distribution indicated that at least 70% of all multiplication processes would be initiated by holes at 75 V reverse bias under 361 nm back illumination. This value increases as either the photon wavelength or bias voltage is reduced.

The current-voltage (*I-V*) characteristics under reverse bias in dark conditions were measured using a HP4155A semiconductor parameter analyzer for different mesa areas and geometries; this primarily allowed for the study of the dark current as a function of the mesa area while giving some insight into the effect of an increase in mesa perimeter for a fixed area. *I-V* curves for circular mesas with increasing areas (shown in Fig. 1) demonstrate a strong dependence of the dark current on the area of the device. The inset of Fig. 1 displays the dark current value at a reverse bias of 70 V for

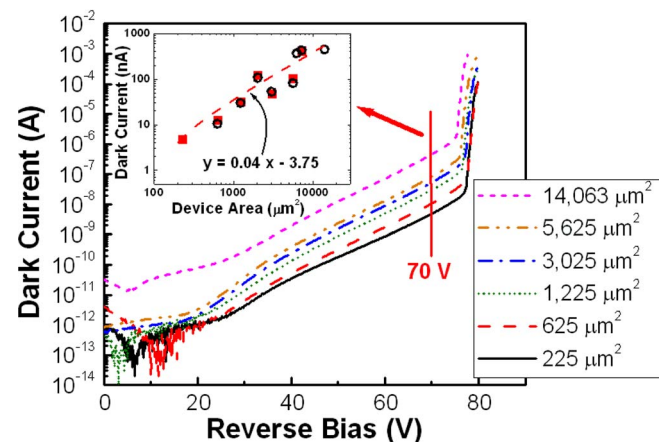


FIG. 1. (Color online) *I-V* curves for circular mesa devices of increasing area. The inset plots the dark current value at 70 V reverse bias for both square (red squares) and circular (open circles) mesas with increasing area.

^{a)}Electronic mail: razeghi@eecs.northwestern.edu

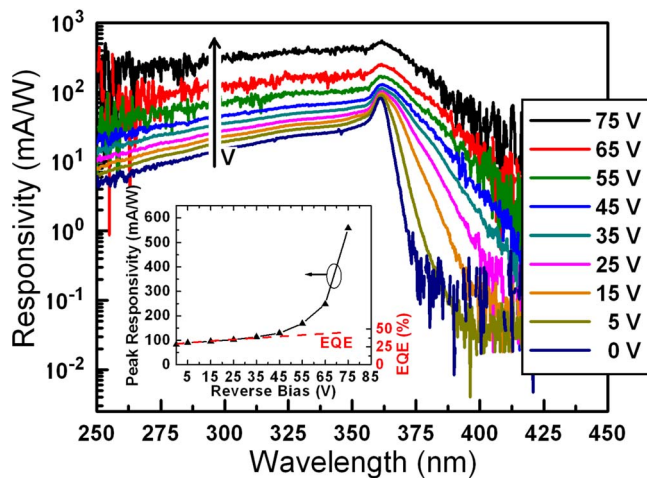


FIG. 2. (Color online) Responsivity measurements with increasing reverse bias. The inset plots the peak responsivity with increasing bias and the extracted external quantum efficiency fit.

increasing device areas for both square and circular mesas, demonstrating a linear increase in dark current with an increase in area. This trend, combined with the negligible differences between the dark current of square and circular mesas of the same area, suggests that the majority of the dark current can be attributed to bulk effects and agrees with the picture of a uniform distribution of higher conductivity threading dislocations across the area of the device.

The series resistances, calculated from the forward bias I - V curves,¹⁰ range from 1.3 k Ω down to 250 Ω with increasing mesa areas from 225 to 25 000 μm^2 . These relatively high values are due to the thin n -GaN layer limiting the lateral conduction. For these back-illuminated devices, it is necessary to compromise between decreasing the thickness of the n -GaN layer in order to maximize device efficiency and increasing the thickness of the n -GaN layer in order to minimize the series resistance. Through previous studies and device modeling, we determined that a 200 nm n -GaN layer was thick enough and that current crowding is not a significant issue, while the absorption losses are low enough to achieve good device efficiencies.

The responsivity with increasing reverse bias (Fig. 2) was measured under back illumination using a xenon arc lamp attached to a monochromator, as described elsewhere.⁷ The devices presented a zero-bias peak responsivity of 82 mA/W at 361 nm, with a significant decay of the response with increasing photon energy, caused by absorption in the n -GaN lateral conduction layer. The absorption coefficient in GaN scales with the photon energy,⁹ making shorter-wavelength photons more likely to be absorbed closer to the AlN interface and thus less likely to diffuse into the depletion region.¹¹ As the bias increases, the response becomes flatter at short wavelengths as the depletion region expands toward the AlN interface. The increasing electric field in the depletion region also makes the long-wavelength cutoff less abrupt at higher voltages due to the Franz-Keldysh effect.¹ At the onset of breakdown, a peak responsivity of 547 mA/W at 361 nm was measured. To better differentiate the effect of this expanding depletion region and the avalanche multiplication in the device, the external quantum efficiency (EQE) of the device was fitted at low voltage, through the use of a one-dimensional finite element model, and extrapolated to high voltages (inset of Fig. 2). Thus, the

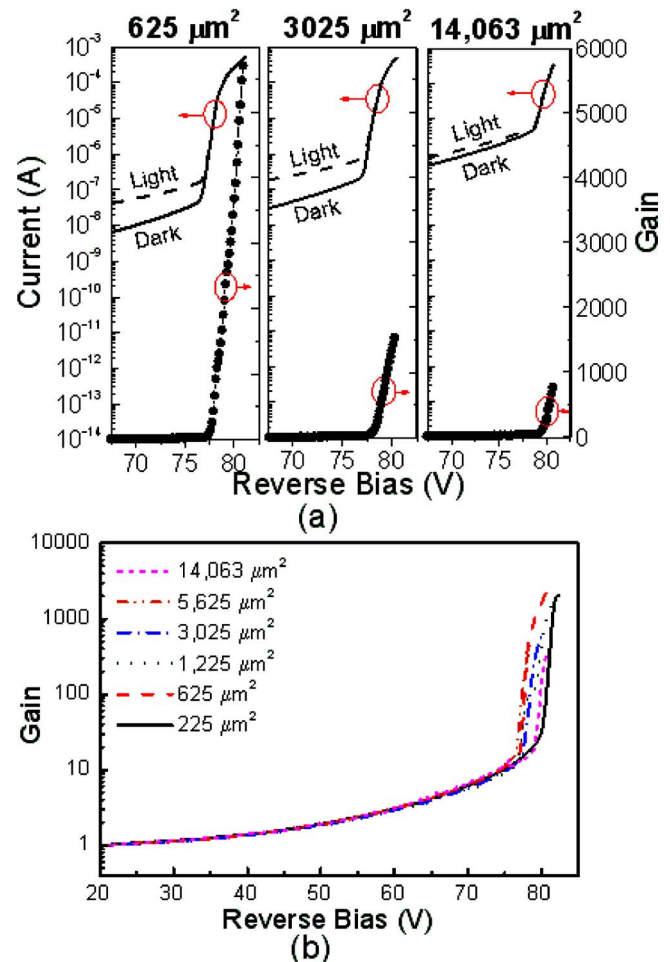


FIG. 3. (Color online) (a) Light current, dark current, and gain curves around breakdown from 625, 3025, and 14 063 μm^2 avalanche photodiodes. (b) Gain vs reverse bias for several mesa areas.

EQE can be understood to increase from 29% at 0 V to 46% at 75 V, for 361 nm photons.

Next, the gain characteristics of several devices were determined by measuring the light and dark I - V curves under reverse bias and subtracting them to obtain the photocurrent. For light current measurements, the back side of the device was illuminated with a frequency-doubled argon ion laser at 244 nm (optical power=76.4 mW/cm²). For each calculated gain curve, the light and dark I - V curves were alternatively measured three times in a row to ensure consistent device operation. The gain is determined by normalizing the photocurrent at the onset of gain ($M=1$); the onset of gain is

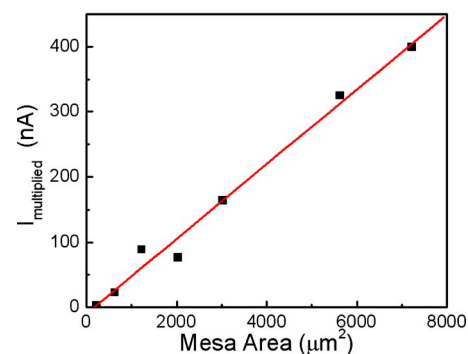


FIG. 4. (Color online) Multiplied current component of the dark current as a function of mesa area.

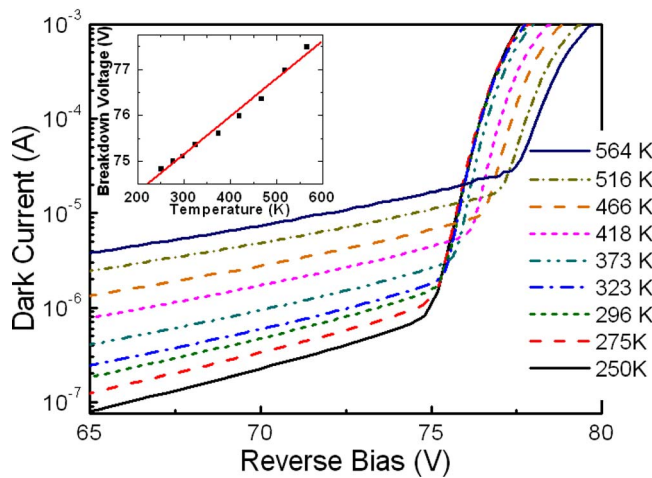


FIG. 5. (Color online) Temperature-dependent evolution of the breakdown from 250 to 564 K for a $14\,063\ \mu\text{m}^2$ device. The inset plots temperature vs breakdown voltage demonstrating a positive thermal coefficient of $+8.3\ \text{mV/K}$.

determined following a similar procedure as used to calculate the EQEs, allowing the establishment of the photocurrent value corresponding to $M=1$.⁷ Figure 3(a) displays the light and dark current curves around breakdown, along with the resulting gain, from circular devices with areas of 625, 3025, and $14\,063\ \mu\text{m}^2$. From these measurements, a very sharp increase in gain at breakdown is observed, and maximum gains of 5700, 1500, and 760, at $\sim 81\ \text{V}$ reverse bias are demonstrated for the 625, 3025, and $14\,063\ \mu\text{m}^2$ devices, respectively. Figure 3(b) displays the gain curves for increasing mesa areas, demonstrating uniform gain behavior with area. There is a slight variation in breakdown voltage; however, there is no trend with area, and therefore this is attributed primarily to material uniformity.

To determine the amount of dark current which experiences avalanche multiplication, the dark current was expressed as $I_{\text{dark}} = I_{\text{multiplied}}M + I_{\text{unmultiplied}}$ and a plot of M vs I_{dark} was utilized to determine $I_{\text{multiplied}}$,¹² which was then plotted as a function of mesa area (Fig. 4). The $225\ \mu\text{m}^2$ mesa has an $I_{\text{multiplied}}$ of 3 nA, which increases linearly up to a value of 400 nA for a mesa area of $7\,225\ \mu\text{m}^2$.

In order to confirm that the gain is the result of avalanche breakdown in the largest area devices, the breakdown characteristics were studied as a function of temperature. Figure 5 displays the dark I - V curves around the breakdown voltage at temperatures ranging from 250 up to 564 K for a $14\,063\ \mu\text{m}^2$ diode, which shows a clear increase in breakdown voltage with temperature. The inset plots the breakdown voltage as a function of temperature, demonstrating a linear behavior with a positive thermal coefficient of $+8.3\ \text{mV/K}$, comparable to other reported values.^{13,14} A similar value was obtained for the $25\,000\ \mu\text{m}^2$ devices, in-

dicating that the thermal coefficient does not appear to scale with area. The general increase in the dark current with temperature is thought to be a thermally activated process. A linear fit to an Arrhenius plot of the dark current at 70 V reverse bias as a function of temperature gave an activation energy of 0.13 eV.

In conclusion, scaling effects in back-illuminated GaN APDs have been studied. With an increase in size, it was found that the dark current increases, indicating bulk leakage as the dominant contribution to the dark current. The responsivity was studied as a function of reverse bias, demonstrating a flatter response at higher voltages. The gain curves were found to be uniform with increasing device area. The multiplied component of the dark current increases linearly with an increase in mesa area. Temperature-dependent measurements were used to confirm the avalanche process in large area devices.

The authors acknowledge the Motorola University Partnership in Research Program for supporting one of the authors (K.M.), the Fulbright Association and the Spanish Ministry of Education and Science for supporting another author (J.L.P.), and the Richter Trust for supporting another author (R.M.).

- ¹K. A. McIntosh, R. J. Molnar, L. J. Mahoney, A. Lightfoot, M. W. Geis, K. M. Molvar, I. McIngalis, R. L. Aggarwal, W. D. Goodhue, S. S. Choi, D. L. Spears, and S. Verghese, *Appl. Phys. Lett.* **75**, 3485 (1999).
- ²J. C. Carrano, D. J. H. Lambert, C. J. Eiting, C. J. Collins, T. Li, S. Wang, B. Yang, A. L. Beck, R. D. Dupuis, and J. C. Campbell, *Appl. Phys. Lett.* **76**, 924 (2000).
- ³A. Osinsky, M. S. Shur, R. Gaska, and Q. Chen, *Electron. Lett.* **34**, 691 (1998).
- ⁴P. Kung, R. McClintock, J. L. Pau, K. Minder, C. Bayram, and M. Razeghi, *Proc. SPIE* **6479**, 64791J (2007).
- ⁵T. Tut, M. Gokkavas, A. Inal, and E. Ozbay, *Appl. Phys. Lett.* **90**, 163506 (2007).
- ⁶R. McClintock, A. Yasan, K. Mayes, P. Kung, and M. Razeghi, *Proc. SPIE* **5732**, 175 (2005).
- ⁷R. McClintock, J. L. Pau, K. Minder, C. Bayram, P. Kung, and M. Razeghi, *Appl. Phys. Lett.* **90**, 141112 (2007).
- ⁸R. McClintock, A. Yasan, K. Mayes, D. Shiell, S. R. Darvish, P. Kung, and M. Razeghi, *Proc. SPIE* **5359**, 434 (2004).
- ⁹J. F. Muth, J. D. Brown, M. A. L. Johnson, Z. Yu, R. M. Kolbas, J. W. Cook, Jr., and J. F. Schetzina, *MRS Internet J. Nitride Semicond. Res.* **4S1**, 1 (1999).
- ¹⁰A. Yasan, R. McClintock, K. A. Mayes, D. J. Shiell, S. R. Darvish, P. Kung, and M. Razeghi, *Proc. SPIE* **5359**, 434 (2004).
- ¹¹E. Monroy, F. Calle, J. L. Pau, F. J. Sanchez, E. Munoz, F. Omnes, B. Beaumont, and P. Gibart, *J. Appl. Phys.* **88**, 2081 (2000).
- ¹²X. Guo, A. L. Beck, X. Li, J. C. Campbell, D. Emerson, and J. Sumakeris, *IEEE J. Quantum Electron.* **41**, 562 (2005).
- ¹³B. Yang, T. Li, K. Heng, C. Collins, S. Wang, J. C. Carrano, R. D. Dupuis, J. C. Campbell, M. J. Schurman, and I. T. Ferguson, *IEEE J. Quantum Electron.* **36**, 1389 (2000).
- ¹⁴J. B. Limb, D. Yoo, J. H. Ryou, W. Lee, S. C. Shen, R. D. Dupuis, M. L. Reed, C. J. Collins, M. Wraback, D. Hanser, E. Preble, N. M. Williams, and K. Evans, *Appl. Phys. Lett.* **89**, 01112 (2006).